Journal of Thermal Analysis and Calorimetry
https://doi.org/10.1007/s10973-023-12244-8

Synergistic effects of P and Si on the flame retardancy in a polymethylsilsesquioxane aerogel prepared under ambient pressure drying

Ye Seo Park[1,2] · Jinkyu Choi[2] · Byeong Seok Kim[2] · Sung-Hyeon Baeck[2] · Sang Eun Shim[2] · Yingjie Qian[1,2]

Received: 18 October 2022 / Accepted: 25 April 2023

Abstract
Polymethylsilsesquioxane (PMSQ) aerogels have been developed for diverse applications owing to their excellent flexibility and hydrophobicity. PMSQ aerogels, however, are limited by their flammability and low thermal stability. In this study, transparent and robust PMSQ aerogels were synthesized using an environmentally friendly flame retardant, 9,10-dihydro-9-oxa-10-phosphaphenanthrene-10-oxide-vinyltrimethoxysilane (DOPO) in a facile one-pot manner and successfully dried under ambient pressure without cracks. Briefly, methyltrimethoxysilane (MTMS) and another synthesized precursor, DOPO-vinyltrimethoxysilane (DOPO-VTMS), where DOPO and VTMS were covalently bonded, were used to prepare a DOPO-VTMS MTMS aerogel via co-hydrolytic condensation. The DOPO-VTMS MTMS aerogel showed excellent flame retardancy with a peak heat release rate of 23.48 W g^{-1}, which is 60% lower than that of the MTMS aerogel. It also exhibited enhanced thermal stability, as confirmed by thermogravimetric analysis, originating from the synergistic effect of P and Si. Furthermore, the compressive strength of the DOPO-VTMS MTMS aerogel was 26 times higher than that of the MTMS aerogel. With superior thermal properties and mechanical robustness, the preparation strategy employed in this study can contribute to the development of PMSQ aerogels for various applications such as thermal insulation for buildings, flame-retardant airspace dust collectors, or fire preventive coatings for fabrics.

Keywords PMSQ aerogel · Flame retardant · Microcalorimeter · Fire hazard

Introduction

Polymethylsilsesquioxane (PMSQ) aerogels have attracted immense interest in the field of silica-based aerogels because they can complement the weak skeleton structure of traditional silica aerogels by replacing silanol groups with methyl groups, thereby reducing the degree of condensation that contributes to shrinkage [1]. Kanamori et al. obtained transparent hydrophobic PMSQ aerogels with improved mechanical properties [2, 3]. Supercritical pressure drying being used to derive the monolith of PMSQ aerogels without cracks or shrinkage requires high pressure and high purity of carbon dioxide [1–3]. Consequently, supercritical pressure drying process is extravagant to manufacture PMSQ aerogels in aspects of safety and cost. In comparison, ambient pressure drying facilitates drying process without any dangerous or complicated conditions. The development of PMSQ aerogel synthesis under ambient pressure drying has progressed for profitable ways by controlling the myriad of variables including of pH, ratio of precursors, surface modification, among others [4–6]. Other studies developed diverse PMSQ aerogels by introducing organo-trialkoxysilanes or organic polymers to enhance their structural stability with functional networks [7, 8]. Since the use of organic carbon-contained precursors will weaken the thermal stability of PMSQ aerogels, studies on the flame retardancy of PMSQ aerogels are needed and currently underway [9, 10].

✉ Sang Eun Shim
seshim@inha.ac.kr

✉ Yingjie Qian
qianyj@ms.giec.ac.cn

Ye Seo Park
yeseopark@pitt.edu

[1] Guangzhou Institute of Energy Conversion, Chinese Academy of Sciences, Guangzhou 510640, People's Republic of China

[2] Department of Chemistry and Chemical Engineering, Education and Research Center for Smart Energy and Materials, Inha University, Incheon 22212, South Korea

Published online: 11 May 2023

In the field of flame-retardant materials, 9,10-dihydro-9-oxa-10-phosphaphenanthrene-10-oxide (DOPO) has been widely studied because of its environmentally friendly nature, and various DOPO derivatives have been determined to be desirable eco-friendly substitutes for use in flammable matrices [11–14]. DOPO neither emits harmful gases during combustion nor remains in the environment, as different from halogenated flame retardants [15]. Further, the synergistic effects of P and Si on flame retardancy have been proven. Si has been well known to be effective for flame retardancy; however, they still have drawbacks despite containing Si. Originally, Si was solely used to influence flame retardancy by forming silica layers as a heat and mass transfer barrier during decomposition, which served as an ''insulating blanket'' that protected the material from flame propagation and delayed the volatilization of decomposition products. [16]. Vasiljevic et al. reported that the use of DOPO-polysilsesquioxanes could improve their transcendent potential for flame retardancy in the gas and condensed phases simultaneously [17]. In the gas phase, the PO radicals emitted from DOPO can react with H and OH radicals during decomposition, resulting in a quenching effect [17]. In the condensed phase, Si and P act as physical barriers that protect the underlying substrate and preclude further flame propagation [17]. Chernyy et al. determined the feasibility of nanosol coatings via the co-hydrolysis co-condensation reaction of DOPO-vinyltrimethoxysilane (VTMS) with a tetraethoxysilane precursor, showing a synergistic flame-retardant effect from combining DOPO and Si [18]. Thus, DOPO and VTMS can be used as flame retardants using methyltrimethoxysilane (MTMS) as a co-precursor in co-hydrolytic condensation.

Herein, we demonstrate the flame-retardant performance of PMSQ aerogels using DOPO-VTMS. As DOPO-VTMS can form cyclic structures in PMSQ aerogels, this PMSQ network can contribute to the high thermal stability of PMSQ aerogels compared to other flame retardants. The purpose of this work was to efficiently lower the flammability of PMSQ aerogels and facilitate the establishment of PMSQ networks through co-hydrolytic condensation reactions with MTMS precursors by introducing DOPO-VTMS. Thermogravimetric analysis (TGA) and micro-combustion calorimetry (MCC) proved that introducing DOPO-VTMS could retard thermal degradation and reduce the peak heat release rate and total heat rate by 67% compared to those of an MTMS aerogel. In addition, the heat rate capacity of the DOPO-VTMS MTMS aerogel was reduced by 60% compared with that of the MTMS aerogel. As a result, not only can the DOPO-VTMS MTMS aerogel be fabricated with good affinity as a part of a PMSQ network, but it can also prevent thermal degradation when burning owing to the synergistic effects of P and Si.

Experimental

Materials

DOPO (> 97%) and VTMS (≥ 98%) were purchased from TCI (Tokyo, Japan). 2,2′-Azobisisobutyronitrile (AIBN, 98%), anhydrous toluene (toluene, 99.8%), and MTMS (98%) were purchased from Sigma-Aldrich (USA). Methyl alcohol (MeOH, 99.5%), ammonium hydroxide (NH_4OH, 28%), and isopropyl alcohol (IPA, 99.5%) were obtained from DUKSAN (South Korea). Hexane (95%) was purchased from DAEJUNG (South Korea).

Synthesis of DOPO-VTMS

Prior to the synthesis, DOPO was stored in a vacuum, and VTMS was protected under an Ar atmosphere. The molar ratio of DOPO, VTMS, and AIBN was 10:10:0.08. First, DOPO and VTMS were dissolved in toluene in a three-neck round flask using a magnetic stirrer equipped with a reflux condenser under an Ar atmosphere at 80 °C. Subsequently, AIBN in toluene was added dropwise at 80 °C for 4 h, and the reaction was carried out at 80 °C for 18 h. Finally, a transparent viscous oil of DOPO-VTMS was obtained and purified at 80 °C using a rotary evaporator to remove the solvent. DOPO-VTMS was further dried under vacuum for 24 h.

Synthesis of MTMS, DOPO MTMS, and DOPO-VTMS MTMS aerogel monoliths

The molar ratio of the precursor, solvent, and catalyst was 1:7:1 for preparing the PMSQ aerogel monolith. A mixture of MTMS (2.5 mL), MeOH (5 mL), and DOPO or DOPO-VTMS (5 mol%) was gently stirred for 30 min at 25 °C, and 1 mL of ammonium hydroxide solution was added dropwise for hydrolytic condensation. Next, an aging step was conducted at 80 °C for 3 d, followed by solvent exchange with IPA and hexane three times per day, and the aged gel was further dried at 60 °C to completely remove any remaining solvent.

Characterization

Proton nuclear magnetic resonance (^{1}H-NMR) spectra were recorded on a Bruker Avance III 400 MHz (USA) spectrometer using $CDCl_3$ as a solvent. Field emission-scanning electron microscopy (FE-SEM) images were recorded using an S-4300E microscope (Japan), and N_2 adsorption–desorption isotherms were recorded on a Brunauer–Emmett–Teller (BET) instrument using a 3-flex instrument (Micromeritics

Instrument Corporation, USA) at 77 K. Fourier-transform infrared (FT-IR) spectra were recorded on a Bruker RFS-100/S (USA) instrument with a universal attenuated total reflection accessory in the wavelength range of 4000 to 500 cm^{-1}. TGA was performed on a TG 209 F3/NETZSCH (Germany), and the samples were heated from 50 to 900 °C at a heating rate of 10 °C min^{-1} with a N_2 flow rate of 30 mL min^{-1}. MCC was carried out using an FAA-PCFC instrument (UK), and the samples were heated from 50 to 900 °C at a heating rate of 1 °C s^{-1} with a N_2 flow rate of 80 mL min^{-1}. After pyrolysis, the combustion temperature was set to 900 °C at an O_2/N_2 flow rate of 20/80 (mL mL^{-1}). Compression tests were performed on the monolithic samples using a universal testing system (DaeKyung, South Korea).

Results and discussion

Synthesis and characterization of DOPO-VTMS

A schematic of the synthesis of DOPO-VTMS is shown in Fig. 1. DOPO is combined with VTMS by breaking the C = C group of VTMS with AIBN as an initiator, resulting in a viscous oil. Subsequently, DOPO-VTMS is reacted with MTMS to produce an aerogel in the sol–gel process. As shown in the ^{1}H-NMR spectrum (Fig. 2), the P–H proton peak at 8.81 ppm disappears after the reaction, indicating that the reaction between DOPO and VTMS is complete. The peaks at 7.24–7.92 ppm (1) confirm the existence of aromatic protons, and the peak at 3.52 ppm (2) results from the protons in the methoxy group. The ratio of the P–H group, aromatic H group (1), and methoxy group (2) is approximately 0:8.00:5.50, suggesting that DOPO-VTMS has been synthesized with little condensation. Proton peaks for the CH_2-CH_2 group can be seen at 0.85 (3) and 2.04 ppm (4). In addition, the peak for the C = C group in VTMS at 6 ppm disappears**,** indicating breakage of the C = C groups [18]. From the FT-IR spectra of MTMS, VTMS, and DOPO-VTMS (Fig. 3), the peaks at 2944 and 2840 cm^{-1} can be attributed to C–H vibrations in aliphatic hydrocarbons, while the VTMS peaks at 1599 and 1410 cm^{-1} can be assigned to C = C vibrations [19]. Double stretching vibrations between 800 and 900 cm^{-1} and peaks at 1078 and 1190 cm^{-1} are attributed to asymmetric Si–O–C vibrations in alkoxysilanes. The peaks at 1267 and 780 cm^{-1} in the MTMS spectrum can be assigned to Si–CH_3 vibrations [20]. The P–H stretching bands at 2384 cm^{-1} and the deformation vibration at 990 cm^{-1} in the DOPO spectrum disappear in the spectrum of DOPO-VTMS after the reaction of DOPO and VTMS [21], which correlates with the disappearance of the proton peak at 8.81 ppm from the ^{1}H-NMR spectrum (Fig. 2). In the spectra of DOPO and DOPO-VTMS, the P–Ph group is represented by bands at 1594 and 1477–1428 cm^{-1} and P = O vibration in the double bands around 1200 cm^{-1} [22]. Bands at 901 and 750 cm^{-1} appear because of the asymmetric stretching vibration of the newly formed P–O–Ph bonds [23].

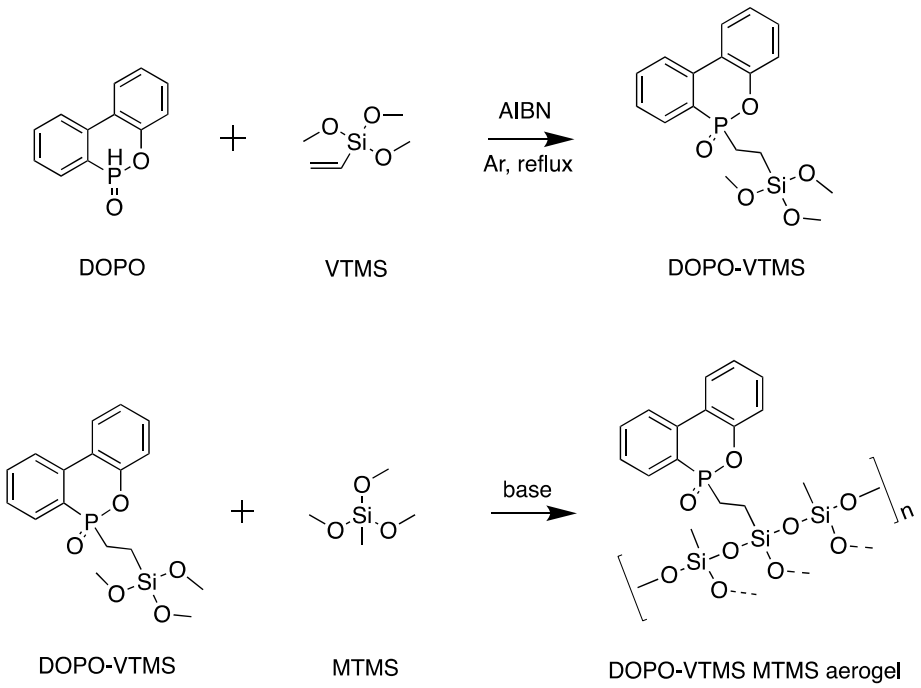

Fig. 1 Schematic of DOPO-VTMS synthesis

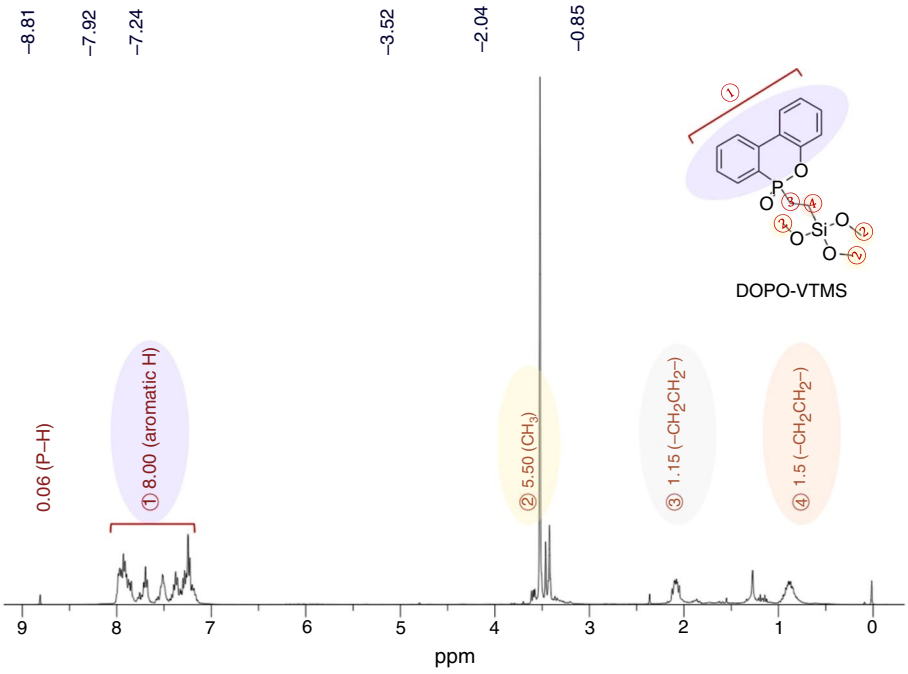

Fig. 2 ^{1}H-NMR spectrum of DOPO-VTMS ($CDCl_3$)

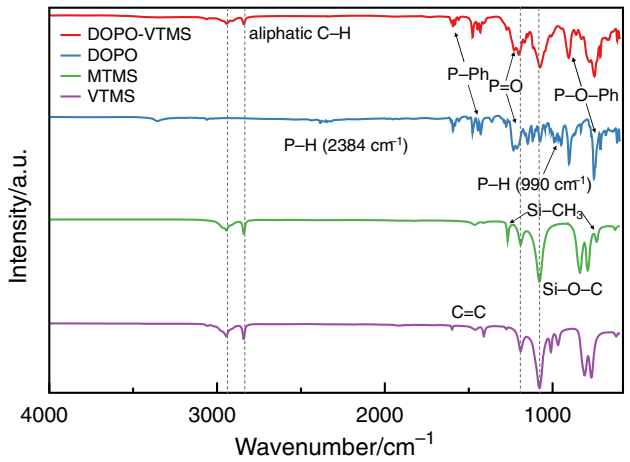

Fig. 3 FT-IR spectra of DOPO-VTMS, DOPO, MTMS, and VTMS (Single column)

Structure and morphology of PMSQ aerogel monoliths

To prepare a flame-retardant aerogel monolith, DOPO and the synthesized DOPO-VTMS were introduced into the PMSQ aerogel and monolithic shape could be achieved under ambient pressure at 60 °C. As shown in Fig. 4, the MTMS (Fig. 4a) and DOPO MTMS aerogels (Fig. 4b) are white, flexible powders, whereas the DOPO-VTMS MTMS aerogel (Fig. 4c) is transparent and more rigid. As the DOPO-VTMS content increases, the transparency of the monolith increases. This is because of the presence of DOPO-VTMS, whose transparent and highly viscous properties affect the transparency of the PMSQ aerogels. Further, co-hydrolytic condensation occurs in the PMSQ network because of the good affinity between DOPO-VTMS and MTMS. There is no structural difference between the MTMS and DOPO MTMS aerogels, and the DOPO-VTMS MTMS aerogel contracts to 50% of its original size. It is presumed that the different kinetic rates of DOPO-VTMS and MTMS influence the sol–gel process and the structural network. In addition, long DOPO-VTMS chains may collapse the structure of PMSQ aerogels. Owing to the delicate synthesis process, a sacrifice of shrinkage is inevitable when constructing a PMSQ aerogel with DOPO-VTMS. In the SEM images shown in Fig. 5, the morphology of the DOPO-VTMS MTMS aerogel (Fig. 5c) is slightly different from that of the others, indicating that the particles agglomerate due to shrinkage; the particle size is approximately 15 nm. In contrast, the MTMS (Fig. 5a) and DOPO MTMS aerogels (Fig. 5b) have 35 nm-sized nanoparticles without agglomeration.

Transparency is mainly related to the scattering of light, which is affected by the pore and particle sizes. It is generally accepted that a smaller pore size leads to lower scattering and higher transparency, as predicted by the Rayleigh scattering equation [24], $I \propto \alpha^6/\lambda^4$, where I is the Rayleigh scattering intensity, α is the pore size, and λ is the wavelength of incident light. The high transparency is attributed to the smallest nanoparticle size in the DOPO-VTMS MTMS aerogel, which exhibits the lowest extent of scattering. N_2 adsorption–desorption isotherms for the aerogels are shown in Fig. 6. Two different types of IUPAC isotherms exist. The MTMS and DOPO MTMS aerogels exhibit a Type

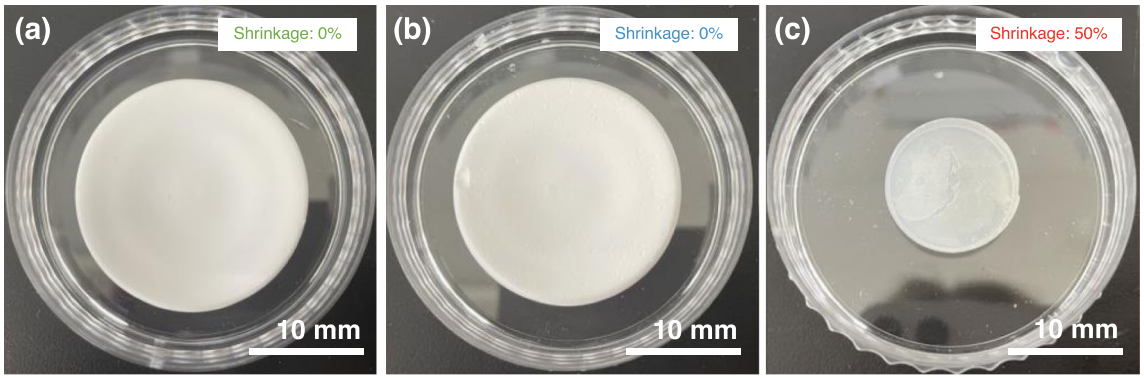

Fig. 4 Digital images of **a** MTMS, **b** DOPO MTMS, and **c** DOPO-VTMS MTMS aerogels

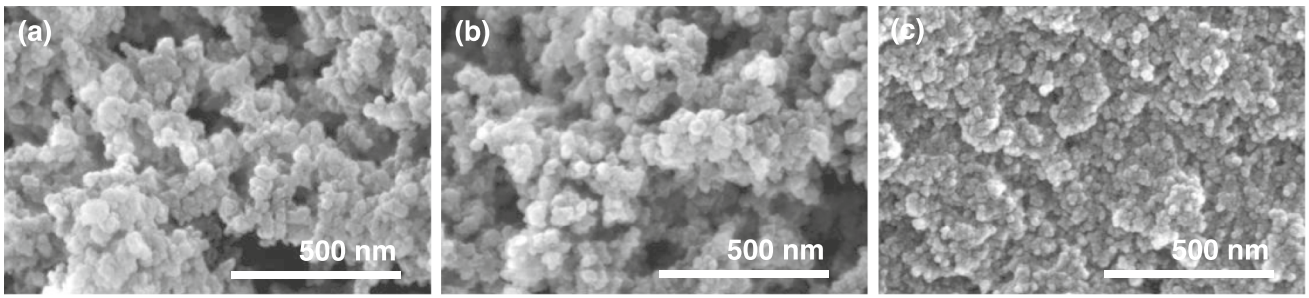

Fig. 5 SEM images of **a** MTMS, **b** DOPO MTMS, and **c** DOPO-VTMS MTMS aerogels

II isotherm as classified by IUPAC, which corresponds to multimolecular BET adsorption behavior with microporous and mesoporous structures, whereas the DOPO-VTMS MTMS aerogel exhibits a Type I isotherm, where unimolecular adsorption is observed with a microporous structure. Although shrinkage occurs in the DOPO-VTMS MTMS aerogel, it has a larger specific surface area than the other two aerogels. The specific surface area (S_{BET}) of the DOPO-VTMS MTMS aerogel is 343.09 $m^2\ g^{-1}$, which is 30% lower than that of the MTMS aerogel. The DOPO MTMS aerogel shows the highest S_{BET} of 661.42 $m^2\ g^{-1}$, which corresponds to the most porous network, as shown in the SEM images. A small amount of DOPO was taken off during the washing step, which might broaden the S_{BET} for the case with voids where DOPO was originally located in the DOPO MTMS aerogel. As a result, the DOPO-VTMS MTMS aerogel has a good S_{BET} with a microporous structure.

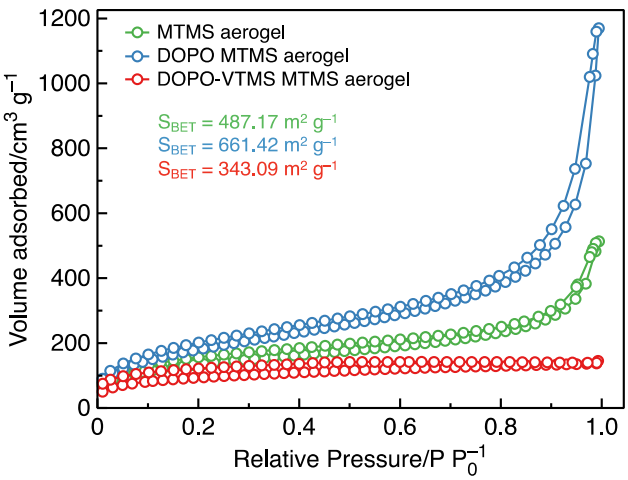

Fig. 6 N_2 adsorption–desorption isotherms of MTMS, DOPO MTMS, and DOPO-VTMS MTMS aerogels (Single column)

Thermal analysis

TGA was performed to investigate the thermal behavior of each aerogel under a N_2 atmosphere. The thermal behavior of the MTMS, DOPO MTMS, and DOPO-VTMS MTMS aerogels differs, as shown in Fig. 7. The DOPO-VTMS MTMS aerogel displays superior thermal stability compared with the other two aerogels. The temperature at 5% mass loss ($T_{95\%}$) of the DOPO-VTMS MTMS aerogel is 476.8 °C, while those of the DOPO MTMS and MTMS aerogels are 349.0 and 336.9 °C, respectively. The DOPO-VTMS MTMS aerogel exhibits the highest $T_{95\%}$, indicating superior thermal stability. The thermal degradation behavior of the MTMS

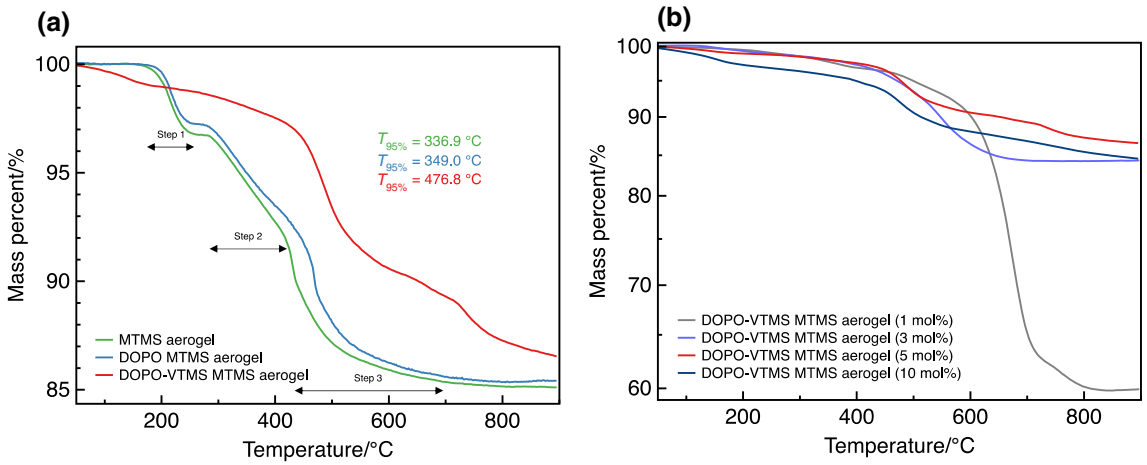

Fig. 7 **a** TG curves of MTMS, DOPO MTMS, and DOPO-VTMS MTMS aerogels and **b** DOPO-VTMS MTMS aerogels with different loadings of DOPO-VTMS

and DOPO MTMS aerogels consists of three degradation steps. In the TG curves for the MTMS and DOPO MTMS aerogels, the first degradation step (Step 1) is ascribed to the evaporation of water and solvents (180–250 °C); Si-CH_3 then decomposes in the range of 250–420 °C (Step 2); and finally, methyl groups cause decomposition up to 700 °C (Step 3) [25]. DOPO affects the thermal stability of the MTMS aerogel by delaying decomposition; therefore, the peaks of the DOPO MTMS aerogels shift slightly to the right. In contrast, DOPO-VTMS exhibits a distinctive thermal behavior that avoids decomposition. It exhibits a sluggish decline of 3% mass loss up to 430 °C, followed by a sharp decline above 430 °C, which corresponds to the thermal behavior of DOPO-VTMS [26]. Given this behavior, it can be assumed that introducing DOPO-VTMS into the PMSQ aerogel would retard the decomposition of Si-CH_3 and methyl groups through the formation of char during the three degradation steps [27]. Furthermore, the char yield of the DOPO-VTMS MTMS aerogel at 900 °C is 86.55%, indicating an improvement in the thermal oxidation resistance compared to that of the PMSQ aerogels. As for the char yield of these aerogels, DOPO-VTMS helps increase char formation and thickens the char layer more than DOPO does. This is mainly due to the synergistic flame-retardant effect of P and Si, attributed to the formation of P honeycomb barriers and additional Si physical barriers [28]. To this end, the strong covalently bonded DOPO-VTMS skeleton helps hinder thermal degradation and improves the thermal stability of the DOPO-VTMS MTMS aerogel. This reasoning can also be applied to the combustion behavior observed in the MCC curve with three similar stages.

Figure 7b shows the thermal stability of the DOPO-VTMS MTMS aerogels at different DOPO-VTMS contents. At 1, 3, and 5 mol% DOPO-VTMS, the $T_{95\%}$ values are similar at 480 °C, while at 10 mol% DOPO-VTMS, $T_{95\%}$ is lower at 400 °C, indicating lower thermal stability despite the introduction of more DOPO-VTMS. The TG curves decrease sharply after these temperatures, particularly for the 1 and 3 mol% DOPO-VTMS. The 1 mol% DOPO-VTMS MTMS aerogel has the lowest char residue of 59.9%, even though it undergoes more serious decomposition than the MTMS aerogel. It is expected that 1 mol% DOPO-VTMS MTMS aerogel cannot maintain its original shape and even affect flame retardancy negatively. The 1, 3, and 5 mol% DOPO-VTMS MTMS aerogels exhibited similar curves up to 420 °C, but the 5 mol% DOPO-VTMS MTMS aerogel shows the best thermal behavior at 420–900 °C. The thermal behavior of the 10 mol% DOPO-VTMS MTMS aerogel seems to have experienced a reverse effect because excessive loading of DOPO-VTMS in the PMSQ aerogel breaks the structure and causes shrinkage. The 5 mol% DOPO-VTMS MTMS aerogel exhibits the highest residue value of 85%. This result leads to the conclusion that 5 mol% DOPO-VTMS is the optimal content for preparing flame-retardant PMSQ aerogels.

Flame-retardant properties

MCC is a convenient and demanding method for limited-size PMSQ aerogels to evaluate flame retardancy during combustion. The combustion heat and vital flammability parameters can be measured directly in standardized tests where the flammability behavior is apparent in the gas and condensed phases under pyrolysis combustion flow [29]. The MCC test was performed at temperatures ranging from room temperature to 900 °C at a heating rate of 1 °C s^{-1} under an N_2 flow of 80 mL min^{-1}, and combustion proceeded at 900 °C. Flammability parameters essential to evaluate the flame-retardant

properties include the heat release rate (HRR), peak heat release rate (pHRR), total heat rate (THR), and heat release capacity (HRC). The HRR is generally defined as the rate of heat generated during decomposition and expresses the quantity of energy released from the fuel. The THR is the area under the HRR curve, and the HRC is the peak HRR divided by the heating rate [30].

In Fig. 8, the HRR curves are plotted versus the pyrolysis temperature, and two peaks are observed during pyrolysis. The heat release behavior corresponds to the specific thermal behavior in each decomposition step. First, some heat release occurs at approximately 200 °C in the HRR curve, corresponding to the loss of solvents and water. The first heat release peaks of the MTMS, DOPO MTMS, and DOPO-VTMS MTMS aerogels occur at 596, 600, and 530 °C, respectively. The gradual slope can be matched to the TG curves, where the curve for the second decomposition step of the DOPO-VTMS MTMS aerogel exhibits a sharp decline, and the curves of the MTMS and DOPO MTMS aerogels decline gently. The second heat release peaks of the MTMS, DOPO MTMS, and DOPO-VTMS MTMS aerogels can be observed at approximately 800 °C, which can be explained by the final decomposition, as seen in the TG curves. There is also a strong correlation between the thermal stability and flame retardancy for multi-component materials. In the HRR curves, the MTMS aerogel has a pHRR value of 57.82 W g^{-1} in the second peak area. The DOPO MTMS aerogel, however, has the highest pHRR value of 69.40 W g^{-1} among the PMSQ aerogels, which implies that merely mixing DOPO and MTMS followed by the preparation of the PMSQ aerogel has an adverse effect on the flame retardancy of the PMSQ aerogel. This result is surprising because it was expected that the HRR might decrease when flame-retardant materials were introduced. Encouragingly, the DOPO-VMTS MTMS aerogel exhibited the lowest pHRR value of 23.48 W g^{-1}. Apparently, DOPO-VTMS can act as a flame-retardant

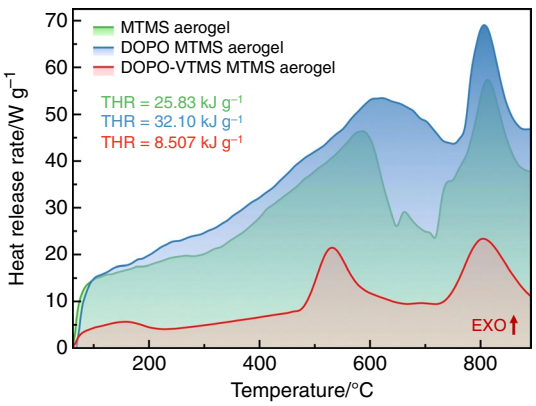

Fig. 8 MCC curves of MTMS, DOPO MTMS, and DOPO-VTMS MTMS aerogels (Single column)

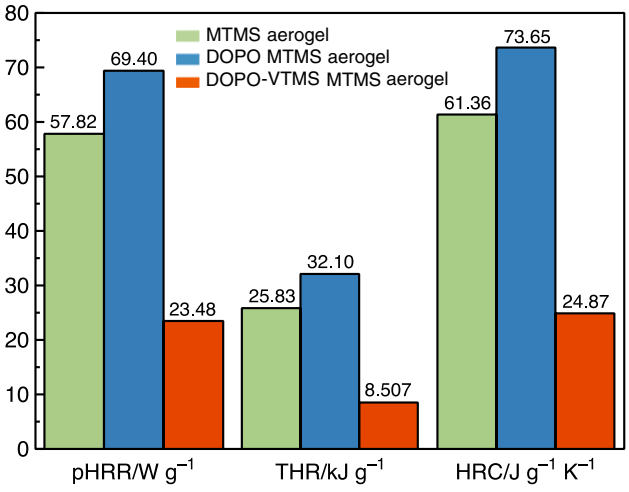

Fig. 9 pHRR, THR, and HRC values of MTMS, DOPO MTMS, and DOPO-VTMS MTMS aerogels (Single column)

agent by reducing the pHRR value by 67% at 800 °C. In this regard, DOPO-VTMS provided flame retardancy and also reduced the total area of heat release during the test. Specifically, the THR values of the MTMS, DOPO MTMS, and DOPO-VTMS MTMS aerogels are 25.83, 32.10, and 8.507 kJ g^{-1}, respectively (Fig. 9). The HRC values of the MTMS, DOPO MTMS, and DOPO-VTMS MTMS aerogels are 61.36, 73.65, and 24.87 J g^{-1} K^{-1}, respectively, (Fig. 9). For the DOPO-VTMS MTMS aerogel, the THR and HRC values are reduced by 67 and 60%, respectively, compared to those of the MTMS aerogel, indicating excellent flame retardancy by introducing DOPO-VTMS into the PMSQ aerogel.

Combustion behavior and char residue morphology

The combustion behavior can be analyzed based on the synergistic effects of P and Si in the gas and condensed phases (Fig. 10). In the gas phase, P suppresses combustion via the quenching effect of free radicals. The DOPO-VTMS structure captures hydrogen radicals, which prevents the further oxidation of volatilized products and inhibits flame propagation [27]. Meanwhile, P has a charring effect since char formation is effectively promoted in the condensed phase [31]. DOPO-VTMS can also form a synergistic char structure of P and Si, while MTMS and DOPO can only form a silica barrier or aromatic char. The char layers containing P and Si successfully prevent the decomposition of the MTMS aerogel. The formation of the P(=O)–O–Si linkage of DOPO-VTMS simultaneously imparts synergistic flame retardancy in the gas and condensed phases [32]. This can increase char formation in the condensed phase because interactions between the DOPO and VTMS, especially in the condensed phase, can induce better flame retardancy than

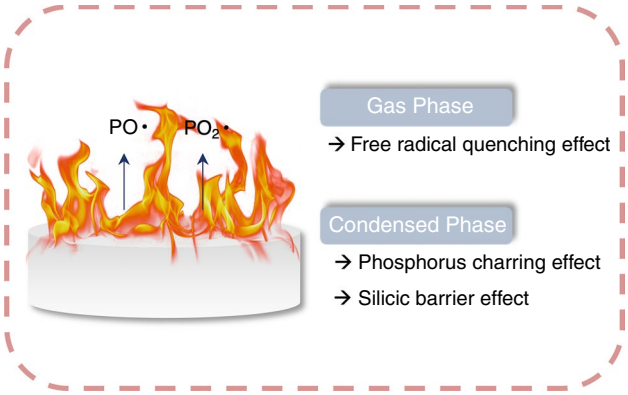

Fig. 10 Combustion mechanism of the DOPO-VTMS MTMS aerogel

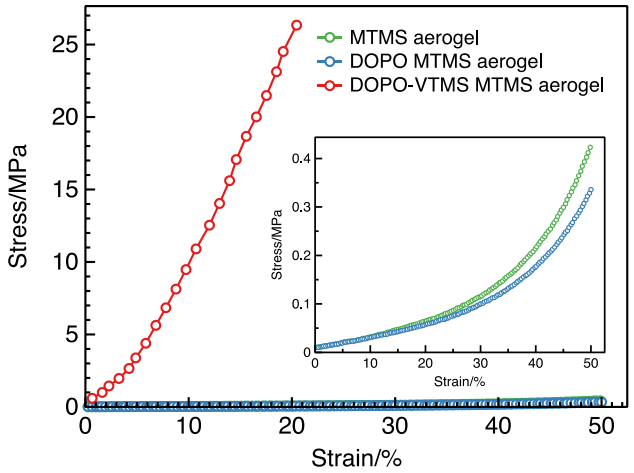

Fig. 12 Stress–strain compression curves of MTMS, DOPO MTMS, and DOPO-VTMS MTMS aerogels (Single column)

when only using Si or P alone [32]. The interactions in the condensed phase play an important role in reinforcing the carbon layers with a robust phenyl and inorganic structure. We surmise that these synergistic flame-retardant effects are due to the P (=O)–O–Si linkage.

Devolatilization is a decomposition process that occurs when volatile compounds are driven out from a hydrocarbon material being heated. It was found that there was no notable char remaining for the MTMS and DOPO MTMS aerogels, whereas the char layers for the DOPO MTMS aerogel were intumescent and firm (Fig. 11). The MTMS aerogel may produce SiO_2 in the gas phase and carbonaceous products in the char layer; however, when PMSQ chemically bonded with DOPO could only interact in the condensed phase [32]. As shown in the SEM images of the burned aerogels (Fig. 11), there are different char morphologies in the PMSQ aerogels. The char becomes less porous and agglomerated in the MTMS (Fig. 11a) and DOPO MTMS (Fig. 11b) aerogels. However, the char morphology of the DOPO-VTMS MTMS aerogel (Fig. 11c) becomes an open system after combustion because of the chemical combination of DOPO and VTMS, leading to the formation of a multi-porous char structure [26]. The strength of the char increases and a thicker char is formed, which is caused by the gaseous products during combustion and the volatilization of these gases. In conclusion, the combustion behavior is strongly enhanced, which is in accordance with the results of the TGA and MCC analyses.

Mechanical properties

A compressive test was conducted with 50% strain to evaluate the mechanical properties of the PMSQ aerogels. The compressive strength is the ability to withstand a compressive force in a cross-sectional area before fracturing. The compressive stress–strain curves of the PMSQ aerogels are plotted in Fig. 12, which shows a difference between the compressive stress–strain curves of DOPO-VTMS MTMS aerogel and those of MTMS and DOPO MTMS aerogels. The stress at fracture of the DOPO-VTMS MTMS aerogel is approximately 26.34 MPa, and 20% of the strain is attained in the compressive test without cracking, which is an unrivaled value compared to the other two aerogels. In contrast, the MTMS and DOPO MTMS aerogels exhibit much lower strengths of 0.42 and 0.34 MPa, respectively. The MTMS and DOPO MTMS aerogels show good

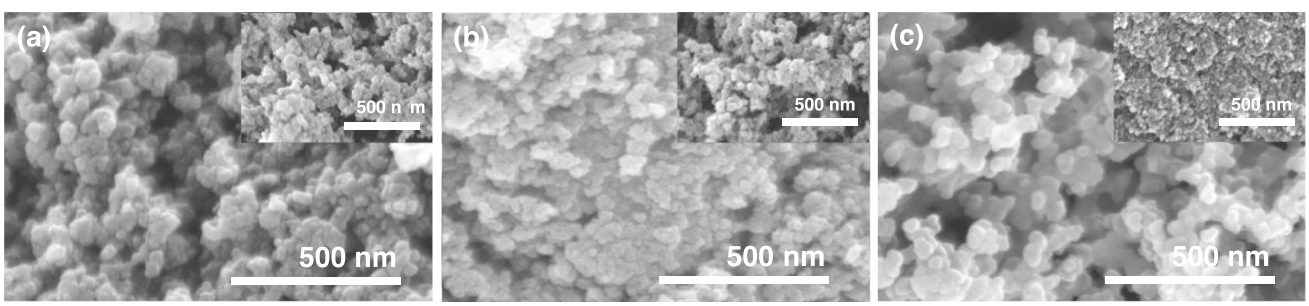

Fig. 11 SEM images of the char residues of **a** MTMS, **b** DOPO MTMS, and **c** DOPO-VTMS MTMS aerogels

flexibility with loading up to 50% stain but are fragile when compressed. Although the cross-sectional area of the DOPO-VTMS MTMS aerogel is much smaller than that of the others owing to its shrinkage, surprisingly, its mechanical strength is the highest among them. The mechanical strength is enhanced by covalent bonding in DOPO-VTMS. The compression modulus is the ratio of the stress to strain during compression. ($E = \sigma/\varepsilon$, where E = compression modulus, σ = strain, and ε = stress) The compression moduli of the MTMS, DOPO MTMS, and DOPO-VTMS MTMS aerogels are 0.007, 0.008, and 0.627 MPa, respectively, i.e., the compressive modulus of the DOPO-VTMS MTMS aerogel is 90 times higher than that of the MTMS aerogel.

Conclusions

In summary, we studied the flame-retardant properties and thermal stability of PMSQ aerogels for fire prevention. A flame-retardant PMSQ aerogel could be prepared simply by ambient pressure drying rather than a more complex process. We analyzed the effects of introducing DOPO and DOPO-VTMS into the MTMS aerogel on its morphology and combustion mechanism and noted remarkable improvements in terms of the thermal and flame-retardant properties. According to the HRR curves, pHRR and THR of the DOPO-VTMS MTMS aerogel were considerably reduced by 67% compared to those of the MTMS aerogel. The HRC of the DOPO-VTMS MTMS aerogel was also reduced by 60% compared to that of the MTMS aerogel. With good affinity between DOPO-VTMS and MTMS in the PMSQ network, the DOPO-VTMS MTMS aerogel exhibited superior flame-retardant properties compared to the DOPO MTMS aerogel. To better understand this, we investigated the combustion behavior of DOPO-VTMS in the gas and condensed phases simultaneously. DOPO derivatives using VTMS could overcome the shortcomings of other flame retardants that are detrimental to human health. In addition, the DOPO-VTMS MTMS aerogel exhibited a compressive strength 26 times higher than that of the MTMS aerogel. Although there was some shrinkage, a transparent, robust, and flame-retardant PMSQ aerogel was obtained. This improved DOPO-VTMS MTMS aerogel could contribute to research applications in fire prevention and the development of flame retardants. As a silica aerogel monolith for fire prevention, it is imperative to fabricate a PMSQ aerogel monolith with excellent flame retardancy.

Acknowledgements This work was supported by the National Research Foundation of Korea (NRF) grant funded by the Korea Government (MSIT) (No. 2020R1A5A1019131).

Author's contribution YSP: Writing—original draft, Formal analysis, Investigation, Visualization. JC: Validation. BSK: Software. S-HB: Resources. SES: Conceptualization, Supervision, Resources. YQ: Supervision, Investigation, Writing—review & editing.

Declarations

Conflict of interest Authors are required to disclose financial or non-financial interests that are directly or indirectly related to the work submitted for publication. Please refer to "Competing Interests and Funding" below for more information on how to complete this section.

References

1. Smith DM, Scherer GW, Anderson JM. Shrinkage during drying of silica gel. J Non-Cryst Solids. 1995;188:191–206.
2. Kanamori K, Aizawa M, Nakanishi K, Hanada T. New transparent methylsilsesquioxane aerogels and xerogels with improved mechanical properties. Adv Mater. 2007;19:1589–93.
3. Kanamori K, Nakanishsi K, Hanada T. Sol-gel synthesis, porous structurer, and mechanical property of poylmethylsilsesquioxane aerogels. J Ceram Soc Japan. 2009;1117:1333–8.
4. Li Z, Cheng X, He S, Huang D, Bi H, Yang H. Preparation of ambient pressure dried MTMS/TEOS co-precursor silica aerogel by adjusting NH_4OH concentration. Mater Lett. 2014;129:12–5.
5. Bi Xu, Cai JY, Finn N, Cai Z. An improved method for preparing monolithic aerogels based on methyltrimethoxysilane at ambient pressure Part I: process development and macrostructures of the aerogels. Microporous Mesoporous Mater. 2012;148:145–51.
6. Cai L, Shan G. Elastic silica aerogel using methyltrimethoxysilane precusor via ambient pressure drying. J Porous Mater. 2015;22:1455–63.
7. Ehgartner CR, Grandl S, Feinle A, Hüsing N. Flexible organofunctional aerogels. Dalton Trans. 2017;46:8809–17.
8. Maleki H, Whitmore L, Hüsing N. Novel multifunctional polymethylsilsesquioxane– silk fibroin aerogel hybrids for environmental and thermal insulation applications. J Mater Chem A. 2018;6:12598–612.
9. Ze Zhang, Wang X, Zu G, Kanamori K, Nakanishi K, Shen J. Resilient, fire-retardant and mechanically strong polyimide-polyvinylpolymethylsiloxane composite aerogel prepared via stepwise chemical liquid deposition. Mater Design. 2019;183:108096.
10. Li L, Xiao Y, Zhang S, Feng J, Jiang Y, Feng J. Lightweight, strong and thermally insulating polymethylsilsesquioxane- polybenzoxazine aerogels by ambient pressure drying. J Sol-Gel Sci Technol. 2021
11. Salmeia KA, Gaan S. An overview of some recent advances in DOPO-derivatives: chemistry and flame retardant applications. Polym Degrad Stab. 2015;113:119–34.
12. Gaan S, Liang S, Mispreuve H, Perler H, Naescher R, Neisius M. Flame retardant flexible polyurethane foams from novel DOPO-phosphonamidate additives. Polym Degrad Stab. 2015;113:180–8.
13. Xie W, Huang S, Tang D, Liu S, Zhao J. Synthesis of a furfural-based DOPO-containing co-curing agent for fire-safe epoxy resins. RSC Adv. 2020;10:1956–65.
14. Kundu CK, Wang X, Rahman MZ, Song L, Hu Y. Application of Chitosan and DOPO derivatives in fire protection of polyamide 66 textiles: towards a combined gas phase and condensed phase activity. Polym Degrad Stab. 2020;176:109–58.
15. Van der Veen I, De Boer J. Phosphorus flame retardants: properties, production, environmental occurrence, toxicity and analysis. Chemosphere. 2012;88:1119–53.

16. Hamdani S, Longuet C, Didier P, Lopez-Cuesta JM, Gananchaud F. Flame retardancy of silicone-based materials. Polym Degrad Stab. 2009;94:465–95.
17. Vasiljevic' J, Jerman I, Jakša G, Alongi J, Malucelli G, Zorko M, Tomšič B, Simončič B. Functionalization of cellulose fibres with DOPO-polysilsesquioxane flame retardant nanocoating. Cellulose. 2015;22:1893–910.
18. Chernyy S, Ulah S, Sørensen G, Tordrup SW, Pedersen PB, Almdal K. DOPO-VTS-based coatings in the realm of fire retardants for cotton textile. J Appl Polym Sci. 2015;132:41955.
19. Qin Z, Li D, Zhang W, Yang R. Surface modification of ammonium polyphosphate with vinyltrimethoxysilane: preparation, characterization, and its flame retardancy in polypropylene. Polym Degrad Stab. 2015;119:139–50.
20. Milenin SA, Khairova RR, Myakkushev VD, Buzin AI, Vasiliev VG, Stoikov II, Muzafarov AM. Synthesis of new organoelement copolymers based on polydimethylsiloxanes and aminophosphonates. J Organomet Chem. 2018;870:110–5.
21. Wang L, Jiang J, Jiang P, Yu J. Synthesis, characteristic of a novel flame retardant containing phosphorus, silicon and its application in ethylene vinyl-acetate copolymer (EVM) rubber. J Polym Res. 2010;17:891–902.
22. Chen W, Liu Y, Xu C, Liu Y, Wang Q. Synthesis and properties of an intrinsic flame retardant silicone rubber containing phosphaphenanthrene structure. RSC Adv. 2017;7:39786.
23. Liu B, Gao X, Zhao Y, Dai L, Xie Z, Zhang Z. 9,10-Dihydro-9-oxa-10-phosphaphenanthrene 10-oxide- based oligosiloxane as a promising damping additive for methyl vinyl silicone rubber (VMQ). J Mater Sci. 2017;52:8603–17.
24. Bangi UKH, Jung IK, Park CS, Baek SS, Park HH. Optically transparent silica aerogels based on sodium silicate by a two step sol–gel process and ambient pressure drying. Solid State Sci. 2013;18:50–7.
25. Shafi S, Zhao Y. Superhydrophobic, enhanced strength and thermal insulation silica aerogel/glass fiber felt based on methyltrimethoxysilane precursor and silica gel impregnation. J Porous Mat. 2020;25:495–502.
26. Wu F, Bao X, Wang J. One-Step reduction of graphene oxide with phosphorus/silicon-containing compound and its flame retardancy in epoxy resin. Polymers. 2021;13:3985.
27. Qian X, Pan H, Xing WY, Song L, Yuen RKK, Hu Y. Thermal properties of novel 9,10-dihydro-9-oxa-10- phosphaphenanthrene 10-oxide-based organic/inorganic hybrid materials prepared by sol-gel and UV-curing processes. Ind Eng Chem Res. 2012;51:85–94.
28. Qian X, Song L, Hu Y, Yuen RKK. Thermal degradation and flammability of novel organic/inorganic epoxy hybrids containing organophosphorus-modified oligosiloxane. Thermochim Acta. 2013;552:87–97.
29. Lyon RE, Walters RN, Stoliarov SI. Screening flame retardants for plastics using microscale combustion calorimetry. Polym Eng Sci. 2007;47:1501–10.
30. Sonnier R, Otazaghine B, Vagner C, Bier F, Six JL, Durand A, Vahabi H. Exploring the contribution of two phosphorus-based groups to polymer flammability via pyrolysis–combustion flow calorimetry. Materials. 2019;12:2961.
31. Jiang Y, Li X, Yang R. Polycarbonate composites flame-retarded by polyphenylsilsesquioxane of ladder structure. J Appl Polym Sci. 2011;124:4381–8.
32. Zhang W, Li X, Fan H, Yang R. Study on mechanism of phosphorusesilicon synergistic flame retardancy on epoxy resins. Polym Degrad Stab. 2012;97:2241–8.